Applied Acoustics 182 (2021) 108265

Contents lists available at ScienceDirect

Applied Acoustics

journal homepage: www.elsevier.com/locate/apacoust

Numerical investigations about the sound transmission loss of a fuselage panel section with embedded periodic foams

Dario Magliacano *, Giuseppe Petrone, Francesco Franco, Sergio De Rosa

PASTA-Lab (Laboratory for Promoting experiences in Aeronautical STructures and Acoustics), Department of Industrial Engineering - Aerospace Section, Università degli Studi di Napoli "Federico II", Via Claudio 21, 80125 Naples, Italy

ARTICLE INFO

Article history:
Received 15 December 2020
Received in revised form 21 June 2021
Accepted 22 June 2021
Available online 3 July 2021

Keywords:
Acoustics
Fuselage
Foam
Sound transmission loss
Design

ABSTRACT

The scope of this paper is to investigate the sound transmission loss of a typical fuselage panel section, as well as to propose solutions based on the inclusion of a periodic pattern inside its foam core, which aim at passively improving the acoustic performance in a mid-high range of frequencies. In detail, a new fuselage panel configuration is numerically studied, starting from the state of the art regarding the acoustic packages based on porous meta-materials. The main novelties of the present work are represented by the application of a meta-core solution inside an acoustic package of aeronautical interest, as well as a systematic investigation of the effects deriving from its geometrical parameters. In order to reach this goal, a numerical model of a fuselage panel section is studied, and the effect of several periodic patterns are simulated; more specifically, twelve configurations are taken into account, each with different radius of the inclusions and number of unit cells along the thickness. For each of these layouts, the mass increase of the so-called meta-core, compared to that of its classical homogeneous counterpart, is estimated, together with the associated mid-band frequency and amplitude of the sound transmission loss peak, which is caused by the additional acoustic modes excited by the periodic nature of the meta-core itself. Results are presented in terms of tables and graphs, which may constitute a good basis in order to perform preliminary design considerations that could be interesting for further generalizations.

1. Introduction

Nowadays, modern urbanization and traffic increase could cause severe noise-induced health damages, such as annoyance, sleep disturbance, or even ischemic heart disease [1], and thus the interest on environment noise control is quickly growing. In general, classical sound absorbing materials may be classified into two different fields: resonators [2] and porous media. Acoustic resonators mainly include perforated panels [3] and/or Helmholtz resonators [4]. These solutions have good performances at low frequencies, but they commonly show the disadvantage of narrow frequency band-gaps [5]. Instead, porous media for acoustic purposes are materials made of channels, cracks or cavities, which let the sound waves to enter the foam, thus dissipating their energy by viscous and thermal losses; these energy consumption dynamics allow sound absorption over wider frequency ranges [6,7]. Anyway, porous media lack of efficiency at low frequencies, compared to their performance at higher ones [8]. Such limitation is generally overcome through the use of multi-layer configurations [9]; in any case, the effects of these solutions always relies on the allowable thickness or on the total mass of the soundproofing configuration [10,11].

An interesting way to improve the efficiency of acoustic packages is constituted by the use of porous media with embedded periodic inclusions [12,13], which exhibit proper dynamic filtering effects that could be advantageous both for the dynamics of the system and its manufacturing aspects. This approach may have several applications in energy, civil and transportation (aerospace, automotive, railway) engineering fields, where space, weight and acoustic comfort still represent critical challenges.

Several studies concerning the acoustic optimization of stiffened [14] and sandwich [15–17] panels may be found in the relevant literature [18,19]. It is well known that the nature of a sandwich core may have a strong influence on the acoustic behavior of aerospace structures [20,21], for both solid foams [22,23] and porous [24,25] or poro-elastic [26–30] layers; in addition, it has been demonstrated that the core geometry plays a relevant role too [31].

In the present work, a new fuselage panel configuration is numerically studied, starting from the state of the art regarding

* Corresponding author.
E-mail address: dario.magliacano@unina.it (D. Magliacano).

https://doi.org/10.1016/j.apacoust.2021.108265
0003-682X/

Nomenclature

c_0	sound speed in air
d	dimension of the unit cell
E	Young modulus
j	imaginary unit
$K = \rho(\frac{\omega}{k})^2$	bulk modulus
k	wave number
n	number of unit cells along the thickness
r	outer radius of the inclusion
t	thickness of the inclusion
T	total thickness of the acoustic package
TL	transmission loss
x, y, z	space coordinates
$Z_c = \sqrt{K\rho}$	characteristic impedance
θ, ϕ	angles of incidence
$\lambda = \frac{2\pi}{k}$	wavelength
ν	Poisson coefficient
$\Pi_{incident}$	incident power
$\Pi_{transmitted}$	transmitted power
ρ	density
ρ_0	density of air
ω	angular frequency

the acoustic packages based on porous meta-materials. Its main novelties are represented by the application of a meta-core solution inside an acoustic package of aeronautical interest, as well as a systematic investigation of the effects deriving from its geometrical parameters. The sound transmission loss may be estimated through different approaches, such as the Transfer Matrix Method (TMM) [32], the Finite Element Method (FEM) [33], the Wave Finite Element Method (WFEM) [9] and the Statistical Energy Analysis (SEA) [34,35], all having their own advantages and limitations [36]. In the context of this research, TMM and FEM are used.

In Section 2, the properties of the studied acoustic package, represented by a typical fuselage multi-layered panel section, are introduced, together with the 3-dimensional finite element (FE) geometries that are investigated in the following sections; also, two preliminary sound transmission loss studies are presented and discussed herein: one with a fixed number of unit cells along the thickness and varying radii of the inclusions, and another with fixed radius of the inclusions and varying number of unit cells along the thickness. Successively, in Section 3, a parametric test campaign is performed for twelve setups, each with different radius of the inclusions and number of unit cells along the thickness; for each of these configurations, the mass increase of the so-called meta-core (the foam core with embedded periodic inclusions), compared to that of its classical homogeneous counterpart, is estimated, together with the associated mid-band frequency and amplitude of the sound transmission loss peak. Some results are presented in terms of tables and graphs, which may constitute a good basis in order to perform preliminary design considerations that could be interesting for further generalizations. In conclusions, in Section 4, the results of this investigation are commented, and some possible future expansions of the present research are evaluated.

2. Application of a periodic foam core in a typical fuselage panel section

In this section, a typical fuselage multi-layered panel section is numerically modeled and studied. For the sake of simplicity, the section is assumed to be plane as shown in Fig. 1.

As described in Fig. 2, from top to bottom, the acoustic package that is the object of this investigation is composed by:

- A layer of air (necessary to excite the system).
- A layer of carbon fiber (representing the fuselage skin).
- A layer of glass wool, with embedded periodic inclusions with the shape of hollow cylinders and made of balsa; the choice of the inclusion geometry and material are made in order to minimize the mass increase respect to the homogeneous counterparts (clearly, the mass increases of the meta-cores are always computed with reference to the volume of the correspondent homogeneous layout). Balsa lumber is very soft and light, with a coarse, open grain. Because its high strength-to-density ratio, balsa is a very popular material for light, stiff structures in model bridge tests, model buildings, and construction of model aircraft.
- A sandwich panel (representing the interior trim), whose skins are made of pre-preg epoxy and with a core made of Divinycell F50. Divinycell F is a class of polyethersulfone-based (PESU)

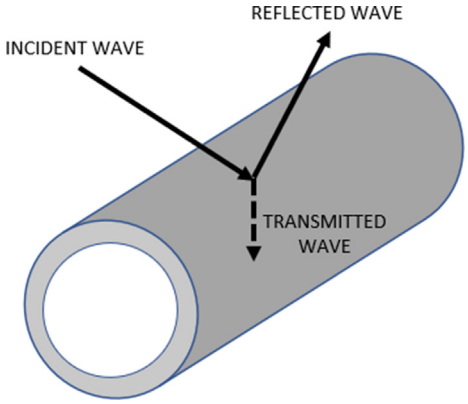

Fig. 1. Scheme of sound incidence, reflection and transmission on a typical fuselage body [37].

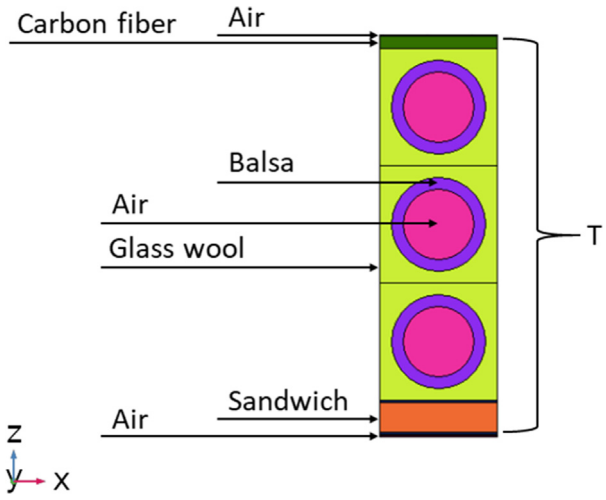

Fig. 2. Example of layering sequence for one of the studied acoustic packages.

recyclable foamed core materials, specifically developed for aircraft interior requirements. It combines lightweight characteristics ("50" represents its density expressed in $[\frac{kg}{m^3}]$) with excellent mechanical properties. It also features low water absorption, resistance to high temperature and chemicals, excellent heat aging behavior as well as inherent flame retardance [38].
- Another layer of air with perfectly matching boundary conditions.

The geometrical and physical properties of the studied acoustic package, consisting of a typical fuselage multi-layered panel section, are reported in Tables 1 and 2, together with a legend of colors with reference to Fig. 2. Properties of air (indicated with pink-colored layers) are: density $\rho_0 = 1.213[\frac{kg}{m^3}]$, speed of sound $c_0 = 342[\frac{m}{s}]$. More specifically, the examined configuration represents the section of a fuselage bay, and thus the presence of stiffeners is not taken into account.

The total thickness of the different studied packages $T = 84.95[mm]$ is kept constant, while their dimensions along x- and y- axes vary; this is irrelevant in this context, since the systems considered herein are always excited by a normal incidence plane wave, and thus the transmission properties of the investigated acoustic package do not depend on the dimensions of its section, but only on that of its thickness (which in this work, as highlighted in Fig. 2, means along the z-axis). For the same reason, it should also be pointed out that, concerning the carbon fiber layer, only the Young modulus along its third direction ($E_2 = E_3 = 8.25 * 10^9[Pa]$) is reported in Table 2 and taken into account in the context of the TMM computations; instead, the FEM analyses account for its anisotropic nature ($E_1 = 141 * 10^9[Pa]$), which anyway does not play a relevant role when the excitation only acts along the third axis.

The glass wool layer is modeled as an equivalent fluid through the Johnson-Champoux-Allard approach [39,40]; the FE implementation and analysis of this kind of materials has already been validated by the authors in their previous works [41], as well as for more complicated di-phasic behaviors [42] through the use of Biot theory of poro-elasticity [43]. In addition, it should be pointed out that the outer radius r and the thickness $t = 0.1 * d$ of the inclusions are expressed as functions of the dimension d of the 3-dimensional cubic unit cell, which is calculated as the total thickness of the glass wool layer divided by the desired number of unit cells. The aforementioned quantities are graphically explained in Fig. 3, on the basis of a single meta-core unit cell; furthermore, Fig. 4 shows some examples of different $\frac{r}{d}$ ratios.

For what concerns the FE implementation, the module "Pressure Acoustics and Frequency Domain" of COMSOL MultiPhysics is used both as modeling environment and numerical solver. For all structures presented in this work, the mesh consists of tetrahedral elements, generated through physics-controlled algorithms that are pre-implemented in the software, which determine a minimum number of six elements per wavelength; as recommended by Mace and Manconi [44], this is a good rule of thumb to ensure a reliable analysis.

Again, since the analyses are carried out considering an excitation consisting of a normal incidence plane wave acting along z-axis, the only fundamental boundary condition to apply is the so-called Perfectly Matched Layer (PML) on the very bottom face of the models: indeed, this represents an artificial absorbing layer for wave equations, commonly used to truncate computational regions in numerical methods in order to simulate problems with open boundaries; this allows the PML to strongly absorb outgoing waves from the interior of a computational region, without reflecting them back into the interior. Such property essentially simulates the interior of the aircraft cabin. On the contrary, boundary conditions applied on faces normal to x- and y- axes are not relevant for analyses with the above-mentioned kind of excitation, since under this condition the waves do not have propagating components along those directions; thus, for the sake of computational simplicity, a Sound Hard Boundary Wall (SHBW) boundary condition is applied herein. Eventually, for different angles of excitation, proper periodic conditions should be used instead. For a plane wave configuration at normal incidence $\theta = \phi = 0$, and thus oriented towards the negative direction of z-axis, the transmission loss is computed as reported in Eq. 1.

$$TL = 10\log_{10}\frac{\Pi_{incident}}{\Pi_{transmitted}}. \quad (1)$$

In the context of this work, the TLs related to the homogeneous (which, obviously, has no inclusions) and the meta-core models are all estimated through a FE implementation of Eq. 1. It should be highlighted that the homogeneous results are also compared with those obtained through WaveSet [45], which is a user-made software, developed in collaboration with Dr. F. Errico [46], allowing a WFEM-based computation of dispersion diagrams and transmission properties of acoustic packages. In particular, for the purposes of the present work, its AcuH toolbox has been used in order to perform a quick and efficient comparison with a TMM-based TL calculation, by generalizing Eq. 2 and Eq. 3 for multi-layered configurations.

$$TL = 10\log_{10}\left(\frac{1}{4}\left| T_{11} + \frac{T_{12}}{\rho_0 c_0} + \rho_0 c_0 T_{21} + T_{22}\right|^2\right), \quad (2)$$

$$\text{with } \begin{bmatrix} T_{11} & T_{12} \\ T_{21} & T_{22} \end{bmatrix} = \begin{bmatrix} \cos(kd) & j\sin(kd)Z_c \\ \frac{j\sin(kd)}{Z_c} & \cos(kd) \end{bmatrix}. \quad (3)$$

Table 1
Properties of JCA-modeled glass wool.

Color	Yellow
Material	Glass wool
Thickness [mm]	75
Porosity	0.99
Tortuosity	1
Airflow resistivity [Pa*s/m^2]	9000
Viscous characteristic length [mm]	0.192
Thermal characteristic length [mm]	0.384

Table 2
Properties of solid layers.

Color	Green	Blue	Orange	Purple
Material	Carbon fiber	Prepreg Epoxy	Divinycell F50	Balsa
Thickness [mm]	2.64	0.48	6.35	0.1*d
ρ **[kg/m̂3]**	1600	1833	50	163
E **[Pa]**	8.25E + 09	3.60E + 09	4.00E + 07	3.86E + 09
v	0.30	0.27	0.32	0.38

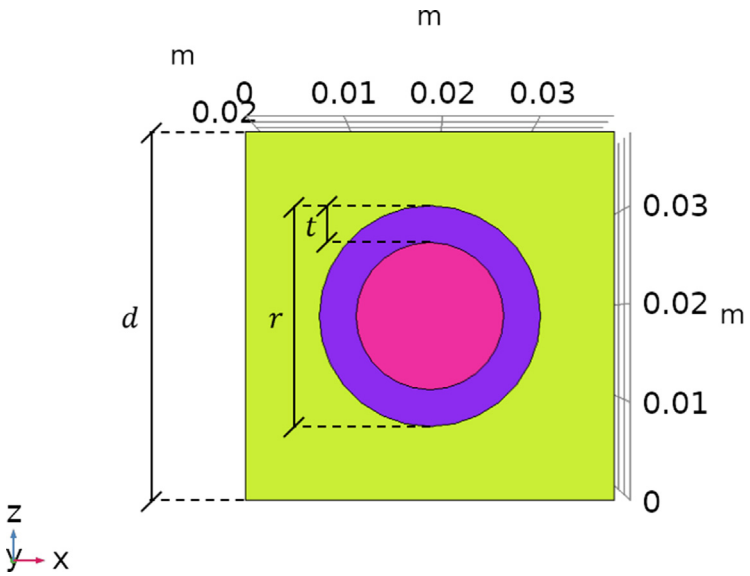

Fig. 3. Example of meta-core unit cell with graphical explanations of r, t and d.

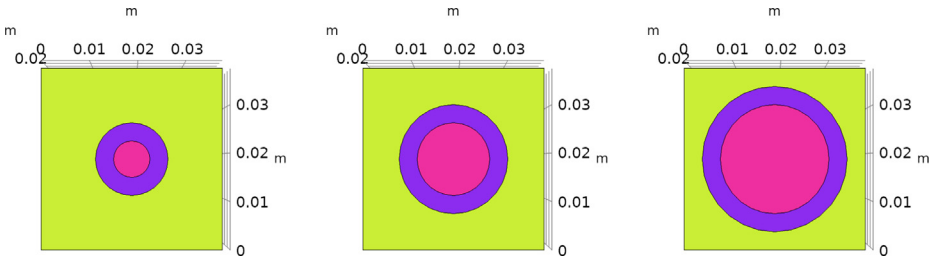

Fig. 4. From left to right, meta-core unit cells with $\frac{r}{d} = 0.2, \frac{r}{d} = 0.3$ and $\frac{r}{d} = 0.4$.

As it may be noted both from Fig. 5 and Fig. 6, the FE-based TL results related to the model having homogeneous layers show an almost perfect agreement with those analytically computed through the TMM; therefore, this comparison plays the role of an analytical validation of numerical results related to the multi-layered configuration without inclusions. It is not conceptually possible to directly perform the same kind of validation also for the meta-configurations, which are anyway endorsed by results shown in Fig. 10.

Two preliminary sound TL studies are presented and discussed herein: one with a fixed number of unit cells along the thickness and varying radii of the inclusions (Fig. 5), and another with fixed radius of the inclusions and varying number of unit cells along the thickness (Fig. 6). As expected, in both cases the meta-core shows a performance peak, related to periodicity effects, when half of the wavelength λ is equal to periodicity dimension d. It should be noted that, since this kind of acoustic resonance still relates on the thickness of the unit cell, it may be challenging to obtain performance peaks at low frequencies, when only a limited thickness is available (as it is in the case of a fuselage bay section); therefore, it is fundamental to realize that the acoustic approach based on meta-cores presented herein may conceptually be scaled also for low-frequency applications, but only when the total available thickness is sufficiently high, or if it is not considered as a model constraint (generally, both conditions are not applicable to solutions in the field of transport engineering). To this aim, some possible solutions are formulated in Section 4.

In Fig. 5, the configuration with three unit cells (which is represented in Fig. 7) is taken into account; it is evident how, by keeping constant the number of unit cells along the thickness of the foam and varying the inclusion radii, the TL peak mid-band frequency shows an almost neglectable shift, while its amplitude increases accordingly with the radius dimension. Instead, as it is clear from Fig. 6, if one keeps the radius of the inclusions constant and let the number of unit cells along the thickness change, both the TL peak mid-band frequency and amplitude vary accordingly with it. More general considerations about the above-described behaviors are found in Section 3.

For the sake of completeness, it should be pointed out that the authors also verified the presence of the so-called air–gap anti-resonance, caused by the presence of the interior trim sandwich panel as predicted by Wilby [47], that anyway is not visible in the figures since it happens at higher frequencies than those analyzed herein.

3. Numerical study for different radii of the inclusions and number of unit cells along the thickness

In this section, a numerical test campaign is performed for twelve configurations, each with different radius of the inclusions and number of unit cells along the thickness. Table 3 shows the number of FE mesh elements for each of the studied configurations, and some example of FE discretization are shown in Fig. 7; a detailed description of classical FE formulation and equations can be easily found in the context of the relevant literature [48,49]. For each of these layouts, the mass increase of the meta-core, compared to that of its classical homogeneous counterpart, is

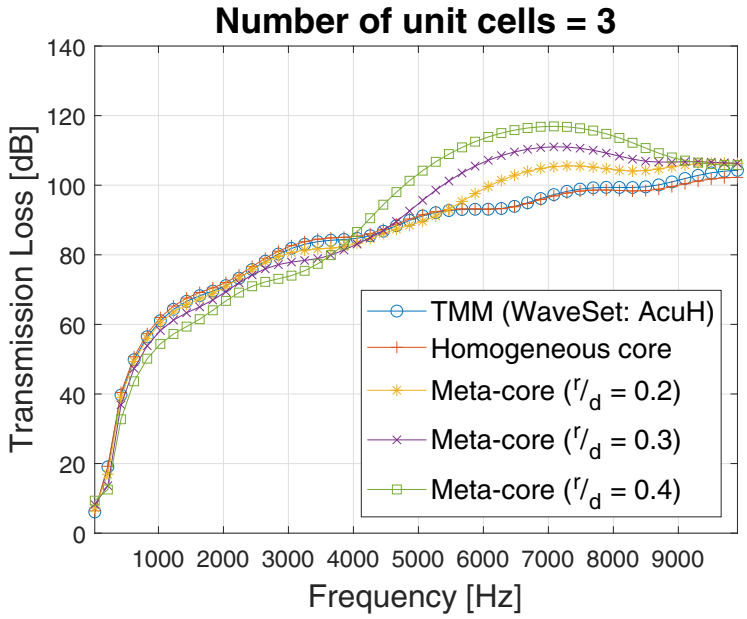

Fig. 5. Transmission loss study with a fixed number of unit cells along the thickness and varying radii of the inclusions.

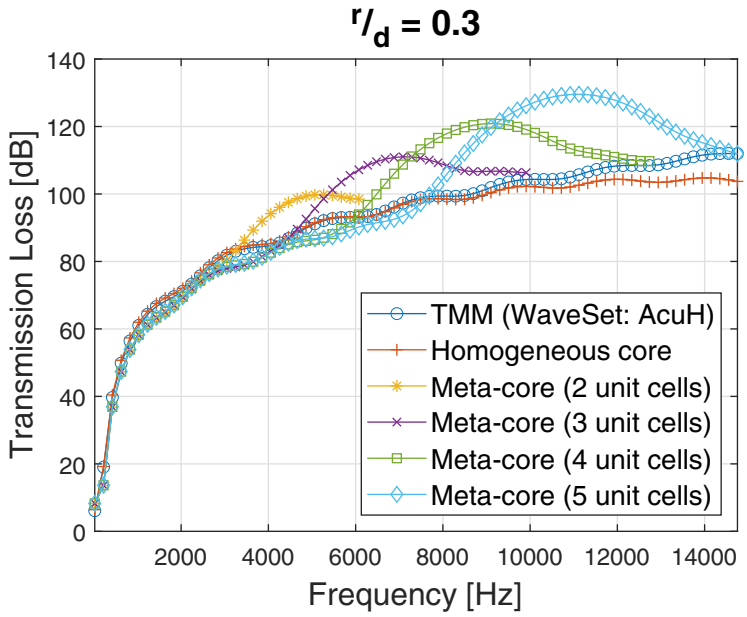

Fig. 6. Transmission loss study with fixed radius of the inclusions and varying number of unit cells along the thickness.

estimated, together with the associated mid-band frequency and amplitude of the sound TL peak.

In addition, a score indicator is arbitrary defined as the ratio between the mid-band amplitude increase of the TL peak and the mass increase, both related to each specific meta-core; this is done with the scope of finding a trade-off parameter that could be meaningful in order to evaluate which configurations appear to be the most advantageous, not taking into account the eventual shift of the peak mid-band frequency. Some results are presented in tabular (Table 4) and graphic (Fig. 8 and Fig. 9) form.

Concentrating on Fig. 9, one may notice that the mass increase basically only depends on the inclusion radius, while the same happens for the frequency of the TL peak but, in this case, with reference to the number of unit cells along the foam thickness. Instead, the amplitude of the sound TL peak seems to depend on both quantities, and it reaches its maximum in correspondence of the highest values of $\frac{r}{d}$ and n.

As a consequence, the above-mentioned score shows a trend meaningful of the fact that both parameters are useful in order to maximize it, but also that n is definitely more weighty in order to reach this goal. For example: if one wants to keep the mass increment as low as possible, and thus needs to minimize $\frac{r}{d}$, through the use of a layout with five unit cells it is possible to obtain a TL peak increase of 15% and a score of 1.09.

The frequency shifts and the TL increases, related to the meta-core configurations that are presented in the context of this work, are only caused by periodicity, and do not depend on the mass increases. In order to verify this statement, a comparison analysis

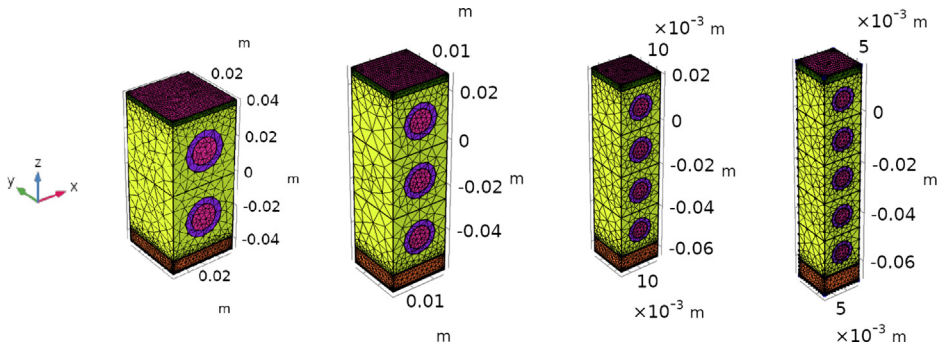

Fig. 7. From left to right, examples of FE discretizations for Configurations 2, 5, 8 and 11 described in Table 3.

Table 3
Number of FE mesh elements for each of the studied configurations.

Configuration	Description	Domain elem.	Boundary elem.	Edge elem.
1	2 cells, r/d = 0.2	64341	17220	1300
2	2 cells, r/d = 0.3	57423	16432	1213
3	2 cells, r/d = 0.4	54473	16264	1202
4	3 cells, r/d = 0.2	40768	11096	1224
5	3 cells, r/d = 0.3	30629	9968	1092
6	3 cells, r/d = 0.4	27972	9694	1065
7	4 cells, r/d = 0.2	28711	8688	1182
8	4 cells, r/d = 0.3	23620	8070	1118
9	4 cells, r/d = 0.4	20190	7576	1061
10	5 cells, r/d = 0.2	24660	7702	1228
11	5 cells, r/d = 0.3	21799	7638	1188
12	5 cells, r/d = 0.4	17611	7038	1117

Table 4
Numerical results of the parametric study, expressed in tabular form.

Configuration	Description	Mass incr.	TL peak freq. [Hz]	TL peak incr.	Score
1	2 cells, r/d = 0.2	13%	4460	8%	0.56
2	2 cells, r/d = 0.3	21%	4460	12%	0.55
3	2 cells, r/d = 0.4	28%	4258	15%	0.53
4	3 cells, r/d = 0.2	13%	6680	10%	0.73
5	3 cells, r/d = 0.3	21%	6478	17%	0.79
6	3 cells, r/d = 0.4	28%	6478	23%	0.83
7	4 cells, r/d = 0.2	13%	8698	12%	0.91
8	4 cells, r/d = 0.3	21%	8698	22%	1.03
9	4 cells, r/d = 0.4	28%	8698	32%	1.13
10	5 cells, r/d = 0.2	13%	10918	15%	1.09
11	5 cells, r/d = 0.3	21%	10716	27%	1.27
12	5 cells, r/d = 0.4	28%	10716	40%	1.44

is carried on, in which the TL curve computed for Configuration 5 of Table 4 is compared with that obtained using completely hollow inclusions with SHBW conditions. In the latter case, which is purely academic, one obtains not an increase, but a reduction of about 5% in terms of mass, which is thus very different from that of Configuration 5; this is essentially due to the fact that the core foam is missing three cylinders of material, respect to the homogeneous case. As it may be noticed from the left part of Fig. 10, results of Configuration 5 and those of SHBW meta-core almost perfectly overlap: this is explained by the fact that the intensity of the acoustic resonance caused by periodicity mainly depends on the impedance mismatch between the foam and the inclusions; therefore, if a material (such as balsa) is able to provide a sufficiently high mismatch value, then the result differences with reference to an ideal case (such as the SHBW one) are practically negligible, regardless of the mass brought by the inclusions themselves. This realization may be quite interesting, since it means that, if one is able to manufacture inclusions made of a material similar to balsa (which already constitutes a good compromise), but with lower density, the mass increases reported in this work could potentially be widely lowered, without experiencing any meaningful drawbacks in terms of TL performances. Moreover, such comparison may also be intended as an additional validation of the numerical results obtained herein, since research studies involving FE-based TL computations of periodic porous materials with internal SHBW conditions are already present in the relevant literature [33].

Furthermore, the right part of Fig. 10 clearly shows the advantage of spending the mass increase in a meta-core solution, rather than in a classical homogeneous one. Indeed, as it may be seen, the homogeneous model with a mass increase of 21% (the same of Configuration 5) provides a light TL increase in the whole frequency band. Anyway, with reference to the typical acoustic requirements of a fuselage panel, it is generally preferred to have a meaningful sound control in a delimited frequency range; to this aim, it is evident that Configuration 5 behaves widely better.

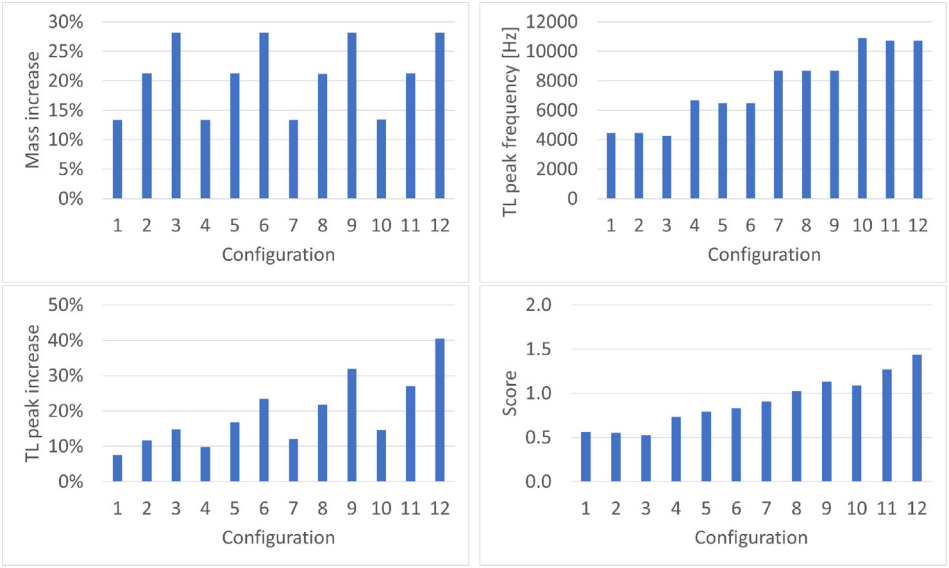

Fig. 8. Numerical results of the parametric study, expressed in the form of bar charts.

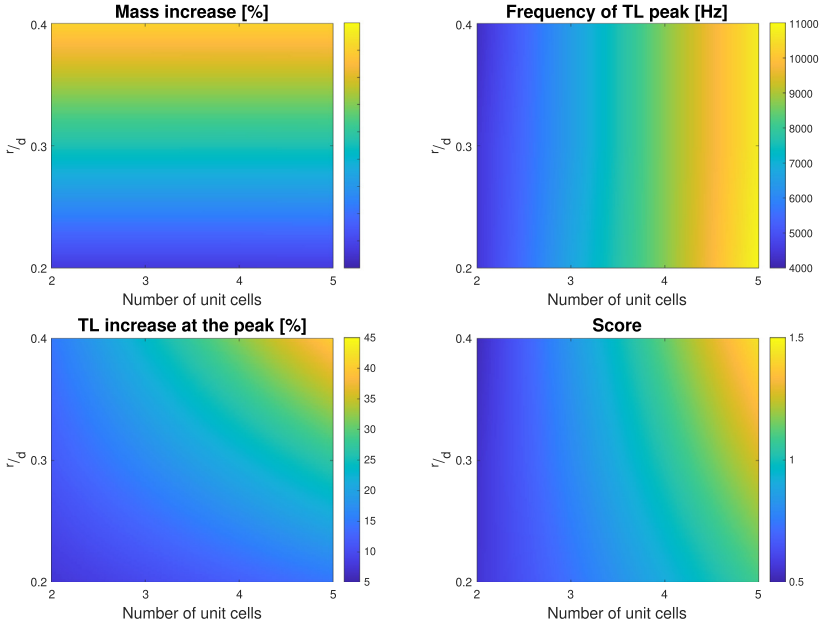

Fig. 9. Numerical results of the parametric study, expressed in the form of color maps.

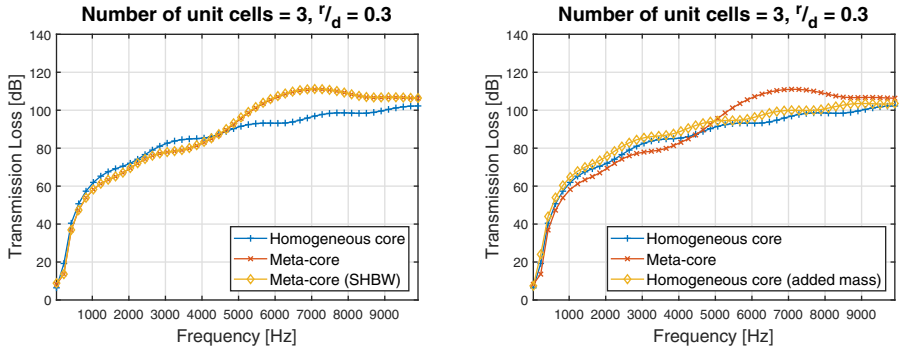

Fig. 10. On the left, TL comparison between Configuration 5 of Table 4 and SHBW meta-core configuration; on the right, comparison between Configuration 5 of Table 4 and a modified homogeneous model with increased mass.

4. Conclusions

In this work, an innovative configuration for a fuselage acoustic package is numerically studied and investigated, with the target of passively improving the acoustic performances in a chosen range of frequencies, and thus in order to introduce some novelties to the state of the art regarding the acoustic packages based on porous meta-materials.

First of all, a numerical model of a fuselage panel section is studied, and the effect of several periodic patterns are simulated.

Successively, twelve setups are taken into account, each with different radius of the inclusions and number of unit cells along the thickness. For each of these configurations, the mass increase of the meta-core, compared to that of its classical homogeneous counterpart, is estimated, together with the associated mid-band frequency and amplitude of the transmission loss peak.

Future works could focus on further reducing the mass increase related to the use of meta-cores, as well as on the analysis of more complex excitation loads. For what concerns potential low frequency applications, the inclusion of periodic Helmholtz resonators in a porous or poro-elastic layer may represent an interesting innovation in the design of sound absorption and insulation packages, since such a configuration may benefit of performance peaks due to both periodic (at mid-high frequencies) and Helmholtz (tunable, and thus potentially at low frequencies) resonances.

CRediT authorship contribution statement

Dario Magliacano: Conceptualization, Formal analysis, Investigation, Validation, Methodology, Writing - original draft, Writing - review & editing. **Giuseppe Petrone:** Conceptualization, Formal analysis, Investigation, Validation, Methodology. **Francesco Franco:** Funding acquisition, Supervision. **Sergio De Rosa:** Funding acquisition, Supervision.

Declaration of Competing Interest

The authors declare that they have no known competing financial interests or personal relationships that could have appeared to influence the work reported in this paper.

Acknowledgments

The authors acknowledge the support of the Italian Ministry of Education, University and Research (MIUR) through the project DEVISU, funded under the scheme PRIN-2017 – grant agreement No. 22017ZX9X4K006.

References

[1] Cao L, Fu Q, Si Y, Ding B, Yu J. Porous materials for sound absorption. Composite Commun 2018;10:25–35. https://doi.org/10.1016/j.coco.2018.05.001.
[2] Zhao XD, Yu YJ, Wu YJ. Improving low-frequency sound absorption of micro-perforated panel absorbers by using mechanical impedance plate combined with helmholtz resonators. Appl Acoust 2016;114:92–8. https://doi.org/10.1016/j.apacoust.2016.07.013.
[3] Yildiz F, Parlar AG, Parlar Z, Bakkal M. Properties of sound panels made from recycled footwear treads. Acta Phys Pol, A 2017;132(3):936–40. https://doi.org/10.12693/APhysPolA.132.936.
[4] Cai C, Mak CM. Noise attenuation capacity of a helmholtz resonator. Adv Eng Softw 2018;116:60–6. https://doi.org/10.1016/j.advengsoft.2017.12.003.
[5] Lv L, Bi J, Wei C, Wang X, Cui Y, Liu H. Effect of micro-slit plate structure on the sound absorption properties of discarded corn cob husk fiber. Fibers Polym 2015;16(7):1562–7. https://doi.org/10.1007/s12221-015-5002-x.
[6] Berardi U, Iannace G. Acoustic characterization of natural fibers for sound absorption applications. Building Environ 2015;94:840–52. https://doi.org/10.1016/j.buildenv.2015.05.029.
[7] Xinzhao X, Guoming L, Dongyan L, Guoxin S, Rui Y. Electrically conductive graphene-coated polyurethane foam and its epoxy composites. Composite Commun 2018;7:1–6. https://doi.org/10.1016/j.coco.2017.11.003.
[8] Groby J-P, Lagarrigue C, Brouard B, Dazel O, Tournat V. Using simple shape three-dimensional inclusions to enhance porous layer absorption. J Acoust Soc Am 2014;136(3):1139–48. https://doi.org/10.1121/1.4892760.
[9] Yang Y, Mace BR, Kingan MJ. Wave and finite element method for predicting sound transmission through finite multi-layered structures with fluid layers. Computers Struct 2018;204:20–30. https://doi.org/10.1016/j.compstruc.2018.04.003.
[10] Weisser T. Acoustic behavior of a rigidly backed poroelastic layer with periodic resonant inclusions by a multiple scattering approach. J Acoust Soc Am 2016;139(2):617–29. https://doi.org/10.1121/1.4940669.
[11] Gaborit M, Dazel O, Göransson P. A simplified model for thin acoustic screens. J Acoust Soc Am 2018;144(1):76–81. https://doi.org/10.1121/1.5047929.
[12] Groby J-P, Wirgin A, De Ryck L, Lauriks W, Gilbert RP, Xu YS. Acoustic response of a rigid-frame porous medium plate with a periodic set of inclusions. J Acoust Soc Am 2009;126(2):685–93. https://doi.org/10.1121/1.3158936.
[13] Xiong L, Nennig B, Aurégan Y, Bi W. Sound attenuation optimization using metaporous materials tuned on exceptional points. J Acoust Soc Am 2017;142(4):2288–97. https://doi.org/10.1121/1.5007851.
[14] Vaicaitis R, Slazak M. Noise transmission through stiffened panels. J Sound Vib 1980;70(3):413–26. https://doi.org/10.1016/0022-460X(80)90309-0.
[15] Franco F, Cunefare KA, Ruzzene M. Structural-acoustic optimization of sandwich panels. J Vibr Acoust, Trans ASME 2007;129(3):330–40. https://doi.org/10.1115/1.2731410.
[16] Li X, Yu K. Vibration and acoustic responses of composite and sandwich panels under thermal environment. Compos Struct 2015;131:1040–9. https://doi.org/10.1016/j.compstruct.2015.06.037.
[17] Yang Y, Li B, Chen Z, Sui N, Chen Z, Saeed M-U, Li Y, Fu R, Wu C, Jing Y. Acoustic properties of glass fiber assembly-filled honeycomb sandwich panels. Compos Part B: Eng 2016;96:281–6. https://doi.org/10.1016/j.compositesb.2016.04.046.
[18] Xin FX, Lu TJ. Sound radiation of orthogonally rib-stiffened sandwich structures with cavity absorption. Compos Sci Technol 2010;70(15):2198–206. https://doi.org/10.1016/j.compscitech.2010.09.001.
[19] Xin FX, Lu TJ. Analytical modeling of wave propagation in orthogonally rib-stiffened sandwich structures: Sound radiation. Computers Struct 2011;89(5–6):507–16. https://doi.org/10.1016/j.compstruc.2010.12.007.
[20] Arunkumar MP, Pitchaimani J, Gangadharan KV, Lenin Babu MC. Influence of nature of core on vibro acoustic behavior of sandwich aerospace structures. Aerosp Sci Technol 2016;56:155–67. https://doi.org/10.1016/j.ast.2016.07.009.
[21] Arunkumar MP, Jagadeesh M, Pitchaimani J, Gangadharan KV, Babu MCL. Sound radiation and transmission loss characteristics of a honeycomb sandwich panel with composite facings: Effect of inherent material damping. J Sound Vib 2016;383:221–32. https://doi.org/10.1016/j.jsv.2016.07.028.
[22] Xin FX, Lu TJ. Effects of core topology on sound insulation performance of lightweight all-metallic sandwich panels. Mater Manuf Processes 2011;26(9):1213–21. https://doi.org/10.1080/10426914.2010.531241.
[23] Petrone G, D'Alessandro V, Franco F, De Rosa S. Numerical and experimental investigations on the acoustic power radiated by aluminium foam sandwich panels. Compos Struct 2014;118(1):170–7. https://doi.org/10.1016/j.compstruct.2014.07.031.
[24] Ghiringhelli GL, Terraneo M, Vigoni E. Improvement of structures vibroacoustics by widespread embodiment of viscoelastic materials. Aerosp Sci Technol 2013;28(1):227–41. https://doi.org/10.1016/j.ast.2012.11.003.
[25] Hung T-C, Huang J-S, Wang Y-W, Lin K-Y. Inorganic polymeric foam as a sound absorbing and insulating material. Constr. Build. Mater. 2014;50:328–34. https://doi.org/10.1016/j.conbuildmat.2013.09.042.
[26] Zhou J, Bhaskar A, Zhang X. Sound transmission through a double-panel construction lined with poroelastic material in the presence of mean flow. J Sound Vib 2013;332(16):3724–34. https://doi.org/10.1016/j.jsv.2013.02.020.
[27] Zhou J, Bhaskar A, Zhang X. The effect of external mean flow on sound transmission through double-walled cylindrical shells lined with poroelastic material. J Sound Vib 2014;333(7):1972–90. https://doi.org/10.1016/j.jsv.2013.11.038.
[28] Liu Y. Sound transmission through triple-panel structures lined with poroelastic materials. J Sound Vib 2015;339:376–95. https://doi.org/10.1016/j.jsv.2014.11.014.
[29] Larbi W, Deü JF, Ohayon R. Vibroacoustic analysis of double-wall sandwich panels with viscoelastic core. Computers Struct 2016;174:92–103. https://doi.org/10.1016/j.compstruc.2015.09.012.
[30] Liu Y, Daudin C. Analytical modelling of sound transmission through finite clamped double-wall sandwich panels lined with poroelastic materials. Compos Struct 2017;172:359–73. https://doi.org/10.1016/j.compstruct.2017.03.024.
[31] Griese D, Summers JD, Thompson L, The effect of honeycomb core geometry on the sound transmission performance of sandwich panels, J Vibr Acoust, Trans ASME 137 (2). doi:10.1115/1.4029043. .
[32] Allard JF, Atalla N. Propagation of sound in porous media: Modelling sound absorbing materials, 2nd Edition. Wiley; 2009.
[33] Magliacano D, Ouisse M, De Rosa S, Franco F, Khelif A, Computation of acoustic properties and design guidelines of periodic biot-modeled foams, Applied Acoustics 168. doi:10.1016/j.apacoust.2020.107428. .

[34] Wang T, Li S, Rajaram S, Nutt SR. Predicting the sound transmission loss of sandwich panels by statistical energy analysis approach. J Vibr Acoust, Trans ASME 2010;132(1):41–7. https://doi.org/10.1115/1.4000459.
[35] Zhou R, Crocker MJ. Sound transmission loss of foam-filled honeycomb sandwich panels using statistical energy analysis and theoretical and measured dynamic properties. J Sound Vib 2010;329(6):673–86. https://doi.org/10.1016/j.jsv.2009.10.002.
[36] Yuan C, Bergsma O, Beukers A. Sound transmission loss prediction of the composite fuselage with different methods. Appl Compos Mater 2012;19(6):865–83. https://doi.org/10.1007/s10443-011-9199-6.
[37] Isaac CW, Pawelczyk M, Wrona S, Comparative study of sound transmission losses of sandwich composite double panel walls, Appl Sci 10 (4). doi:10.3390/app10041543. .
[38] Divinycell f - basf aerospace materials and technologies. URL: https://aerospace.basf.com/divinycell-f.html. .
[39] Johnson DL, Koplik J, Dashen R. Theory of dynamic permeability and tortuosity in fluid-saturated porous media. J Fluid Mech 1987;176(1):379–402. https://doi.org/10.1017/S0022112087000727.
[40] Champoux Y, Allard JF. Dynamic tortuosity and bulk modulus in air-saturated porous media. J Appl Phys 1991;70(4):1975–9. https://doi.org/10.1063/1.349482.
[41] Magliacano D, Ouisse M, Khelif A, De Rosa S, Franco F, Atalla N, Collet M, Computation of dispersion diagrams for periodic porous materials modeled as equivalent fluids, Mechanical Systems and Signal Processing 142. doi:10.1016/j.ymssp.2020.106749. .
[42] Magliacano D, Ahsani S, Ouisse M, Deckers E, Petrone G, Desmet W, De Rosa S, Formulation and validation of the shift cell technique for acoustic applications of poro-elastic materials described by the biot theory, Mechanical Systems and Signal Processing 147. doi:10.1016/j.ymssp.2020.107089. .
[43] Biot M. Mechanics of deformation and acoustic propagation in porous media. J Appl Phys 1962;33(4):1482–98. https://doi.org/10.1063/1.1728759.
[44] Mace BR, Manconi E. Modelling wave propagation in two-dimensional structures using finite element analysis. J Sound Vib 2008;318:884–902. https://doi.org/10.1016/j.jsv.2008.04.039.
[45] Waveset - engineering innovation. URL: https://wavesetconsulting.com. .
[46] Errico F, Flow-induced vibrations and noise of periodic structural systems, Ph. D. thesis, Ecole Centrale de Lyon (France) (2020). .
[47] Wilby JF. The prediction of interior noise of propeller-driven aircraft: A review. SAE Trans 1983;92(3):75–90. https://doi.org/10.4271/830737.
[48] Xing C, Zhou C, Finite element modeling of crack growth in thin-wall structures by method of combining sub-partition and substructure, Engineering Fracture Mechanics doi:10.1016/j.engfracmech.2018.03.023. .
[49] Isaac CW, Wrona S, Pawelczyk M, Roozen NB, Numerical investigation of the vibro-acoustic response of functionally graded lightweight square panel at low and mid-frequency regions, Compos Struct 259. doi:10.1016/j.compstruct.2020.113460. .